Auxiliary Material

Collective behavior of antagonistically acting kinesin-1 motors

Cecile Leduc, Nenad Pavin, Frank Jülicher and Stefan Diez

Methods

All the chemicals were purchased from Sigma, except specifically mentioned.

Polarity-marked MTs
Seeds were polymerized in BRB80 (80 mM PIPES/KOH pH 6.9, 1 mM EGTA, 1 mM $MgCl_2$) with 1 mM GMPCPP, 1 mM $MgCl_2$, and 1.4 mg/mL Alexa-488-labeled porcine tubulin (ratio 1:3 labeled/unlabeled) for 30 minutes at 37°C. After centrifuging at 100,000 g seeds were elongated with 0.08 mg/mL tubulin (1:1:2 Alexa-488 : Rhodamin : unlabeled) in presence of 1 mM GMPCPP, 1 mM $MgCl_2$ and 14 μM NEM (N-ethylmaleimide)(previously quenched with 8 mM B.M.E. for 10 min) for 12 min at 37°C. Tubulin was purchased from Cytoskeleton Inc. (Denver, CO).

Gliding assays
The glass surface of a flow cell (volume about 10 μL) was first incubated for 5 min with a solution of 0.5 mg/mL casein in BRB20 (20 mM PIPES/KOH pH 6.9, 1 mM EGTA, 1 mM $MgCl_2$). The chamber was next incubated with a solution of 20 nM kinesin-1 (wild type, full length purified as in [1]) for 5 minutes, giving rise to a surface density of about 500 molecules/μm^2 (estimation following Vale et al [2]). Then, motility solution containing 1 mM or 10 μM ATP (Roche, ordering number 10519979001, batch 12957226), an oxygen scavenger system (20 mM D-glucose, 110 μg/mL glucose oxidase, 20 μg/ mL catalase and 10 mM DTT), 0.2 mg/mL casein and 0.05 μM MT-doublets was injected. The MT-doublet solution was prepared by incubation of about 1 μM MTs (polarity marked or not) and 1 μM anti-β-tubulin (Qiagen) for 5 minutes. All experiments were performed in BRB20 because we found that the ionic strength of this buffer lead to the formation of stable MT-doublets (due to an enhanced strength of the bonds between anti-β-tubulin and the MTs) as well as to reliable motility. We tuned the ratio of MTs to antibodies as well as the total concentrations of MTs and antibodies to mainly form MT-doublets as compared to bundles of three and more MTs. We obtained about 20% MT-doublets, about 80% single MTs and a negligible quantity of bundles with more than two MTs ($n = 223$, 8 experiments). In gliding motility assays, we observed about three times more parallel than antiparallel doublets (total of 43 doublets analyzed in 8 experiments). Presumably, this difference—far from the expected equal probability—stems from the fact that antiparallel doublets often separated before being observed. In those cases, the forces applied by the antagonistic motors might have been stronger than the cross-linking forces exerted by the antibodies. We observed that in the case of parallel doublets (Figure A1), the velocities v at 1 mM ATP were similar to the velocity of individual MTs (v_0): $v/v_0 = 0.97 \pm 0.05$ (mean $\pm$ SD, $n = 28$), with $v_0 = 0.44 \pm 0.07 \mu m/s$. The velocity v_0 was measured in each time-lapse movie. In particular, for every experimental point represented in Fig. 2, v_0 was evaluated by averaging the velocities of all individual MTs (typically around 5) present in the same field of view as the corresponding doublet. Overall, the variation in v_0 was found to be below 5%.

Imaging and analysis
Fluorescent images of MT-doublets were observed by epi-fluorescence using an Axiovert 200M microscope (Zeiss, Oberkochen, Germany), a 100x (N.A. 1.45) oil-immersion objective, an optovar 1.6 and an Andor Ixon DV 897 EMCCD camera (Andor, Belfast, U.K.). Time-lapse movies were acquired by alternation between the green (FITC) and the red channels (TRITC). The alignement of the two color images was obtained by image analysis, knowing the velocity of the MT-doublets. To cut the MT-doublets, we employed a laser cutter associated with a confocal microscope (OLYMPUS FV-1000) using the laser lines 405 nm (diode laser) and 488 nm (argon laser). Image analysis was performed using Metamorph software.

Measuring kinesin-1 processivity

To measure the kinesin processivity, and to obtain a numerical value for the detachment rate at zero load, single molecule stepping assays were performed using quantum dots (same protocol as in [5]). Performing the experiments under the same conditions as in the doublet gliding assays, 1x10 $^{-15}$ mol of kinesin-1 was incubated with 5x10 $^{-15}$ mol of biotinylated anti-his antibodies and 25x10 $^{-15}$ mol of streptavidin-coated quantum dots (655 nm emission wavelength) for 5 minutes. This mix was diluted 40 times and then injected into the flow chamber. The glass surface was previously coated with dimly rhodamin-labeled MTs and passivated with F127 [3]. Time lapse movies were acquired (1 frame/s) (see Fig. A8 for a typical kymograph). The traveled distance of all the molecules were summed up and divided by the number of detachments in order to get an estimation of the processivity [5]. We obtained a run length of L = 58 ± 25 μm (mean ± SE, n= 5 detachments for 36 molecules evaluated). The corresponding detachment rate was $\omega_0 = v_0/L = 0.01 \pm 0.005$ s^{-1} (mean ± SE). As already noted in the main text, this detachment rate is unexpectedly low. The detachment rate of Drosophilia kinesin-1 was measured previously to be about 0.5 s^{-1} [10]. Our buffer conditions are almost identical. They contain less salt, but this alone could only explain a decrease in the detachment rate by a factor of about 2 [10, 11]. Nevertheless, we consistently observed a detachment rate about 25 times smaller. We also measured such a low detachment rate under the same buffer conditions using truncated GFP-labeled rat kinesin-1 molecules [5], which indicates that our finding is not construct dependent. We therefore attribute this low detachment rate to our experimental conditions specified in particular by the utilized tubulin and/or the specific batch of ATP. We are currently investigating this issue in molecular details.

Physical description of collective dynamics

Probability density for a motor to be attached to the MT and to have extension y is denoted $p_{\rm a}(y)$. This probability density obeys kinetic Eq. (1) in the main text. In steady state $\partial_t p_{\rm a} = 0$ we have:

$$\frac{dp_{\rm a}}{dy} = -\frac{1}{v+v_{\rm m}}\left[\frac{dv_{\rm m}}{dy}\,p_{\rm a} + \omega_0\exp(k|y|/f_{\rm c})\,p_{\rm a} - \omega_{\rm on}Q_{\rm d}A\exp\left(-\frac{ky^2}{2k_{\rm B}T}\right)\,p_{\rm d}\right] \tag{A.1}$$

Here $v_{\rm m} = v_{\rm m}(f)$ is force-velocity relationship for a single motor. Eq. (A.1) has singularity when denominator $v + v_{\rm m}$ has zero value; in this case motor is in steady state with extension $y_{\rm st}$. Note that this singularity vanishes when term which describes velocity fluctuations $D_{\rm a}\frac{d^2p_{\rm a}}{dy^2}$ is included [6]. The homogeneous equation associated to equation (A.1)

$$\frac{dp_{\rm a}}{dy} + \frac{1}{v+v_{\rm m}}\left[\frac{dv_{\rm m}}{dy} + \omega_0\exp(k|y|/f_{\rm c})\right]p_{\rm a} = 0 \tag{A.2}$$

can be solved by expansion in a Laurent series around $y_{\rm st}$. In the vicinity of this singularity the probability density $p_{\rm a}$ can be approximated by

$$p_{\rm a} \simeq \alpha_0^{\mp}(\mp y \pm y_{\rm st})^r \tag{A.3}$$

for $y < y_{\rm st}$ and $y > y_{\rm st}$, respectively. It can be shown that $r = -\frac{\omega_0\exp(ky_{\rm st}/f_{\rm c})}{dv_{\rm m}/dy} - 1$. Hence, the singularity in the density profile appears when $\omega_0\exp(ky_{\rm st}/f_{\rm c}) < -dv_{\rm m}/dy$. For all force-velocity relationships used in this paper $r > -1$ and thus all integrals converge to $\int_{y_{\rm st}}^{y_{\rm st}\pm\delta} p_{\rm a}dy = \pm\alpha_0^{\pm}\delta^{r+1}/(r+1)$.

We calculate the probabitlity density $p_{\rm a}(y)$ for $y < y_{\rm st} - \delta$ and $y > y_{\rm st} + \delta$ by numerically solving Eq. (A.1). In the vicinity of the singularity $y > y_{\rm st} - \delta$ and $y < y_{\rm st} + \delta$ the solution is given by Eq. (A.3). By using numerical solutions of $p_{\rm a}$, we calculate coefficients $\alpha_0^{\pm} = p_{\rm a}(y_{\rm st} \pm \delta)\ /\ \delta^r$.

Influence of the MT-overlapping region

We did check for a possible influence of length of the overlapping region on the experimentally results. We find that the doublet velocity curves are the same not only for different MT lengths but also for different overlap lengths. All data collapse onto a single curve even though the overlap lengths vary. In principle, there could have been an effect of overlap length if there were a competition for motors by the two MTs in the overlap region. The observed data collapse, however, shows that such a competition is not important in our experiments and that the presence of the second MT does not influence the number of motors binding to the first MT in the overlap region.

This idea is supported by the finding that the usual extension of a single motor is in the range of 20 nm [9] while the distance between the centerlines of the cross-linked MTs is in the range of 35 nm (25 nm for twice the MT radius plus the dimension of the crosslinking antibodies). We therefore do not consider this competition in our theory.

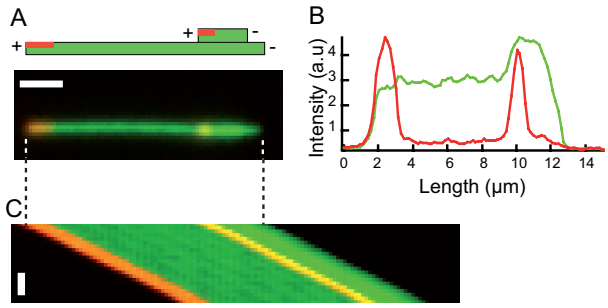

Figure A1: Gliding motiliy assay of parallel polarity-marked MT-doublets. (A) Dual-color epifluorescence image of a parallel doublet, bar 2 μm. (B) Fluorescence intensity profiles in the red and the green channels. (C) Kymograph illustrating the doublet movement, vertical scale bar, 1 min.

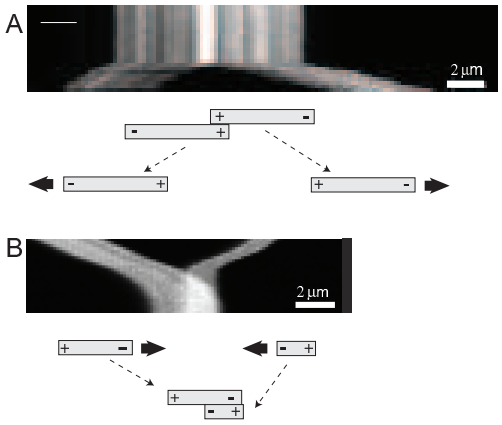

Figure A2: Separation and formation of antiparallel MT-doublets. (A) Kymograph and schematics showing the separation of MTs from an antiparallel doublet. Because the doublet was composed of MTs with approximately equal lengths, the doublet did initially not move. After spontaneous separation, presumably triggered by competing motor forces, both single MTs recovered their full velocity. Bar, 2 μm, total time: 38 s. (B) Kymograph and schematics showing the formation of an antiparallel doublet. Two fast moving MTs (coated with antitubulin antibodies) happened to meet with opposite polarities. The formed doublet moved with significantly lowered velocity. Bar, 2 μm, total time: 1 min 10 s.

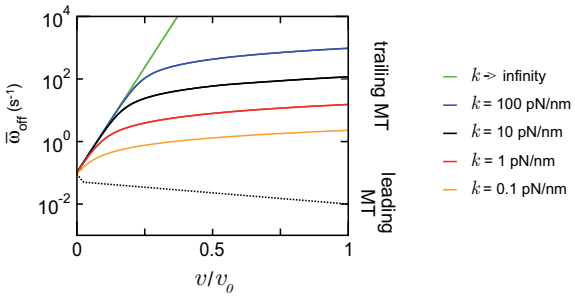

Figure A3: Influence of the motor stiffness on the system behavior. Average rates of motor detachment from the leading and trailing MT $\bar{\omega}_{\rm off} = Q_a^{-1}\int_{-\infty}^{\infty}\omega_{\rm off}(y)p_{\rm a}(y)dy$ as function of the normalized doublet velocity. Colors indicate different values of k. For detachment from the leading MT, all curves fall onto each other and are therefore represented by a dotted line.

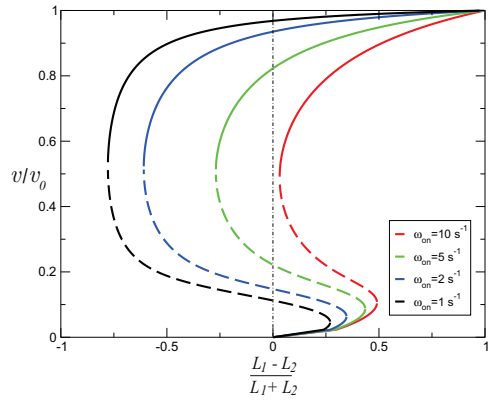

Figure A4: Influence on the attachment rate, ω_{on}. Normalized doublet velocities ($v_0 = 0.44$ μm/s) as functions of the relative MT length differences for different values of the attachment rate, ω_{on}. While the slow branch is rather unchanged, the fast branch widens and its slope decreases upon an increase in ω_{on}. Besides ω_{on}, all other parameters are defined in the caption of Fig. 3 in the main text. Note that the green curve corresponds to the black curves in Figs. 3B and C in the main text.

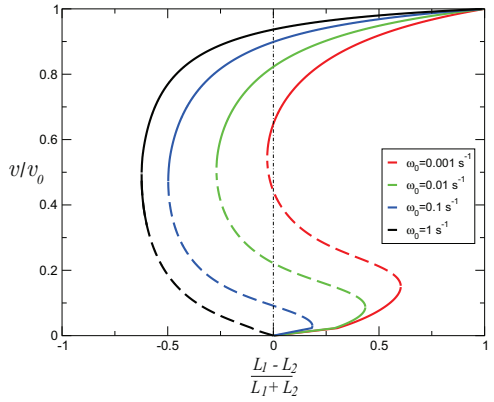

Figure A5: Influence on the detachment rate, ω_0. Normalized doublet velocities ($v_0 = 0.44$ μm/s) as functions of the relative MT length differences for different values of the detachment rate at zero load, ω_0. The detachment rate at zero load plays a limited role on the shape of the doublet velocity curve: the faster the motors detach, the more narrow the slow branch becomes, while the fast branch remains rather unchanged. Besides ω_0, all other parameters are defined in the caption of Fig. 3 in the main text. Note that the green curve corresponds to the black curves in Figs. 3B and C in the main text.

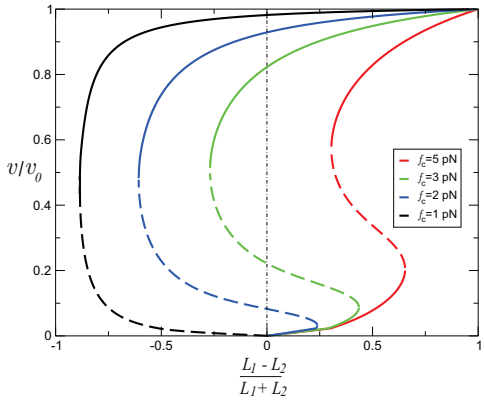

Figure A6: Influence on the characteristic force, f_c. Normalized doublet velocities ($v_0 = 0.44$ μm/s) as functions of the relative MT length differences for different values of the characteristic force, f_c. The characteristic force f_c has, compared to the other parameters, the most significant influence on the doublet velocity curve. It determines the existence of the slow and the fast branch, as well as the slope of the fast branch. Besides f_c, all other parameters are defined in the caption of Fig. 3 in the main text. Note that the green curve corresponds to the black curves in Figs. 3B and C in the main text.

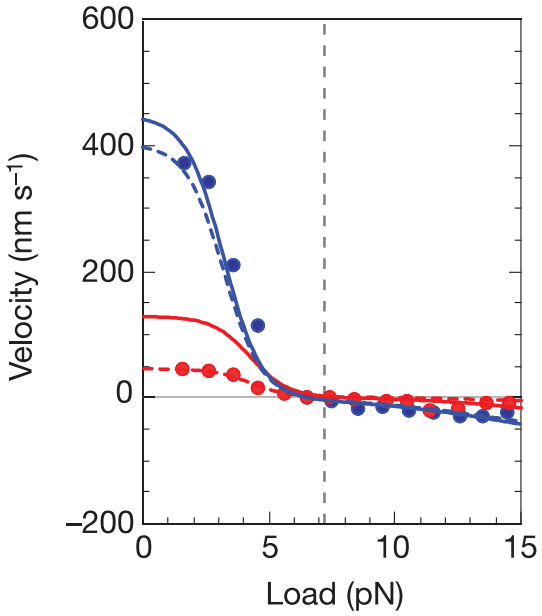

Figure A7: Approximation of the force-velocity relationships at saturating (1 mM) ATP (blue) and low (10μM) ATP concentration (red), using the model of Kolomeisky and Fisher [7]. The force-velocity relation of single motors is given by

$$v_{\mathrm{m}}(f) = d\frac{u_0u_1 - w_0w_1}{u_0 + w_0 + u_1 + w_1} \tag{A.4}$$

where forward rates (u_0, u_1) and backward rates (w_0, w_1) are given by

$$u_0(f) = u_0(0)\exp(-fd^+/k_{\mathrm{B}}T) \tag{A.5}$$
$$u_1(f) = u_1(0) \tag{A.6}$$
$$w_0(f) = w_0(0)\exp(fd^-/k_{\mathrm{B}}T) \tag{A.7}$$
$$w_1(f) = w_1(0) \tag{A.8}$$

The parameters for blue and red curves in table below were chosen to reproduce our experimental doublet velocity curves in Fig. 2 A and B in the main text, respectively.

parameter	blue line	dashed blue line	red line	dashed red line
$u_0(0)$	5000 s^{-1}	4500 s^{-1}	6000 s^{-1}	2100 s^{-1}
$u_1(0)$	56 s^{-1}	50.4 s^{-1}	16 s^{-1}	5.6 s^{-1}
$w_0(0)$	0.5 s^{-1}	0.45 s^{-1}	0.04 s^{-1}	0.014 s^{-1}
$w_1(0)$	10 s^{-1}	9 s^{-1}	5 s^{-1}	1.75 s^{-1}
$k_{\mathrm{B}}T/d^+$	0.75 pN	0.75 pN	0.75 pN	0.75 pN
$k_{\mathrm{B}}T/d^-$	3 pN	3 pN	2.5 pN	2.5 pN
d	8 nm	8 nm	8 nm	8 nm

To check the reasonability of the assumptions thereby made, we also plotted for comparison the experimental data from Carter and Cross [4] (blue and red circles) and our curves scaled by factors of 0.9 (dashed blue line) and 0.35 (dashed red line). These scalings are made in order to match velocities at zero force measured in Ref. [4] at high ATP concentration and at low ATP concentration.

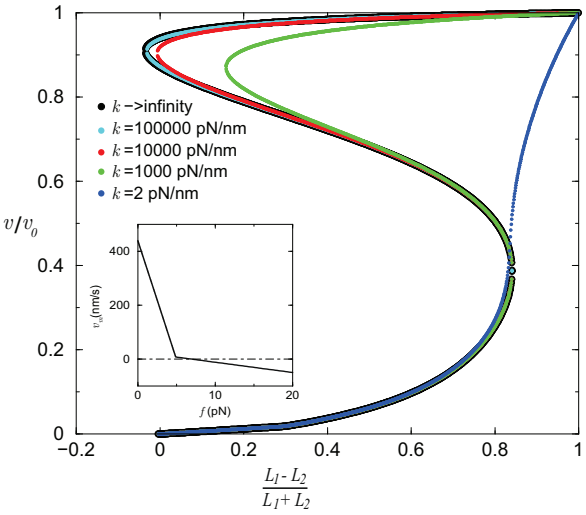

Figure A8: The asymptotic property of the model. The model introduced in the main text can be simplified by assuming that the motor is attached to the substrate by stiff linked which does not stretch. In this case, the doublet and motor velocities are of the same magnitude but opposite sign $v = -v_m(f)$, and the kinetic equation (1) from the main text is replaced by

$$\frac{dQ_{\rm a}}{dt} = \omega_{\rm on}\,(1 - Q_{\rm a}) - \omega_{\rm off}(f)\,Q_{\rm a}. \qquad \text{(A.9)}$$

The average force exerted by a single motor on the left MT is then given by $\bar{f}(v) = Q_{\rm a}\ f$. The experimental data (normalized doublet velocity vs. relative MT length difference) at high ATP concentration (fig. 2A) are best predicted with the following parameters: f_c=9.5 pN, $\omega_{\rm on} = 5\ s^{-1}$ and $\omega_0 = 0.01\ s^{-1}$. Using these same parameters in the full model, and by varying the motor stiffness k from 2 to 100 000 pN/nm, we observe that: (i) when k tends to infinity we go back to the simple, (ii) for finite value of k the agreement with experimental data is improved. We note that to obtain a prediction of the experimental data with the simple model, we needed to use parameters (especially f_c, which appears in an exponential) far from data published previously [8]. We note that, with the simple model, the predictions for the doublet-velocities were also much less robust than with the full model.

Figure A9: Determining the processivity of kinesin-1 motors. Typical example of a kymograph obtained from stepping motility assays using single kinesin-1 molecules attached to quantum dots, under the same experimental conditions (salt, ATP, oxygen scavenger etc.) as used in the doublet experiments. Bar, 1 μm. Total time: 40 s.

[1] D. L. Coy, M. Wagenbach and J. Howard (1999) *J Biol Chem* 274: 3667-3671
[2] R. D. Vale, F. Malik and D. Brown (1992) *J Cell Biol* 119: 1589-1596
[3] J. Helenius, G. Brouhard, Y. Kalaidzidis, S. Diez and J. Howard (2006) *Nature* 441: 115-119
[4] N. J. Carter and R. A. Cross (2005) *Nature* 435: 308-312
[5] V. Varga, C. Leduc, V. Bormuth, S. Diez and J. Howard (2009) *Cell* 138: 1174-1183
[6] S. W. Grill, K. Kruse and F. Jülicher, Phys. Rev. Lett. **94**, 108104 (2005)
[7] A.B. Kolomeisky and M. Fisher (2007) *Annu. Rev. Phys. Chem.* 58: 675-695
[8] M. J. Schnitzer, K. Visscher and S. M. Block (2000) *Nat Cell Biol* 2: 718-723
[9] J. W. Kerssemakers, J. Howard, H. Hess and S. Diez (2006) *PNAS* 103: 15812-15817
[10] R. D.Vale, T. Funatsu, D. W. Pierce, L. Romberg, Y. Harada, T. Yanagida (1996) *Nature* 380: 451-453
[11] K. S. Thorn, J. A. Ubersax, and R. D. Vale (2000) *J Cell Biol* 151: 1093-1100